Received: 14 February 2024 | Revised: 12 March 2024 | Accepted: 31 March 2024

DOI: 10.1002/pc.28439

RESEARCH ARTICLE

Polymer COMPOSITES WILEY

Wood flour and hazelnut shells polylactide-based biocomposites for packaging applications: Characterization, photo-oxidation, and compost burial degradation

Marilena Baiamonte[1,2] | **Marco Rapisarda**[3] | **Maria Chiara Mistretta**[1,2] | **Giuseppe Impallomeni**[3] | **Francesco Paolo La Mantia**[1,2] | **Paola Rizzarelli**[3]

[1]Dipartimento di Ingegneria, Università di Palermo, Palermo, Italy

[2]INSTM, Consorzio Interuniversitario Nazionale per la Scienza e Tecnologia dei Materiali, Firenze, Italy

[3]Istituto per i Polimeri, Compositi e Biomateriali (IPCB) – SS di Catania, Consiglio Nazionale delle Ricerche (CNR), Catania, Italy

Correspondence

Francesco Paolo La Mantia, Dipartimento di Ingegneria, Università di Palermo, Viale delle Scienze, 90128 Palermo, Italy.
Email: francescopaolo.lamantia@unipa.it

Paola Rizzarelli, Istituto per i Polimeri, Compositi e Biomateriali (IPCB) – SS di Catania, Consiglio Nazionale delle Ricerche (CNR), via P. Gaifami 18, 95126 Catania, Italy.
Email: paola.rizzarelli@cnr.it

Funding information

Sicilian Region PO FESR 2014–2020

[Correction added on 12 August 2025, after first online publication: The copyright line was changed.]

Abstract

In this work, polylactide (PLA) was loaded with wood flour (WF) or hazelnut shells (HSs) (10% and 20% of fillers). The matrix and biocomposites were fully characterized from a mechanical and rheological point of view to test their processability and mechanical performance. Compost burial degradation test (30 days), with or without a prior photo-oxidation step, assessed their biodegradability after an outdoor application, and was monitored by weight loss (WL). The viscosity of the biocomposites was lower than that of the matrix and this unusual result can be attributed to a limited adhesion between the PLA and fillers. Both fillers increased the elastic modulus but decreased the tensile strength and elongation at break. As for the weathering, the degradation of PLA was mostly due to hydrolytic chain scission due to the presence of humidity. Resistance of PLA to UV irradiation improved in presence of both the two fillers. Their lignocellulosic nature was responsible for this behavior. Both fillers induced a high resistance and lower degradation in compost: WL percentages of virgin PLA was about 26%, biocomposites with 20% of WF or HS showed WL of about 10% and 14%, respectively. Photo-oxidation (36 h with condensation cycle) increased the compost degradation rate of both biocomposites and WL of PLA with 20% of WF or HS were about 15% and 21%, respectively, after 30 days.

Highlights

- Poor adhesion between the matrix and fillers reduced the biocomposites viscosity.
- Fillers increased the elastic modulus but decreased the properties at break.
- Both fillers improved the resistance of PLA to UV irradiation.
- Biocomposites showed a lower susceptibility to compost degradation than PLA.
- Photo-oxidation increased the compost degradation rate of biocomposites.

Marilena Baiamonte and Marco Rapisarda contributed equally to this work.

KEYWORDS

biocomposites, biodegradable polymers, biomass biowaste, polylactide, polymer degradation

1 | INTRODUCTION

The term "biocomposites" has been used for polymer composites having as an inert phase a biomass. Both biodegradable bio-based polymers and fossil-derived polymers were used for these polymer systems. The objective of all these types of biocomposites is to reduce the environmental impact of the polymers. In the case of bio-based, biodegradable matrices, these polymer systems are carbon neutral and at the end of their life are biodegraded. Then, one of the most important tools to reduce the environmental impact of polymers is the use of bio-based, biodegradable polymers. These polymers are prepared from monomers derived from biomasses and, at the end of their life, are biodegraded and/or composted. The same final fate occurs for the natural filler. Promoted by national and international environmental agreements, recent trends aim at use biomass wastes. In this context, the employ of biocomposites can be a noteworthy help in an effective conversion towards a circular economy.

Many books or chapter of books,[1–5] reviews,[6–10] and papers[11–39] have been published on the preparation, characterization, degradation, and recycling of biocomposites. Both traditional fossil-derived polymers[10–15] and biodegradable bio-based polymers[16–39] have been used as matrices; many different fillers like wood flour (WF), cornstarch, cellulose, rice husk flour, sisal, flax, agricultural, marine waste, and so forth were employed. In general, the matrices become more rigid with increasing the content of filler, but this is accompanied by a reduction of the tensile strength and of the elongation at break. Moreover, the size of the fillers plays an important role. In fact, viscosity and mechanical properties improve with decreasing the dimensions of the filler particles. As for the resistance of the matrix with respect to thermal and photo-oxidative degradation and biodegradation, different results have been found depending on the nature of the filler.[15–25] Averous and Boquillon[15] found that the addition of cellulose improves the thermal resistance without significant effect on the post-processing stability. Kim et al.[16] investigated biocomposites of polybutylene succinate (PBS) with WF and rice husk flour. The fillers improve the degradation of PBS during natural soil burial test. Batista et al.[22] studied the soil degradation of a biodegradable matrix (poly (hydroxy butyrate-co-hydroxy valerate), PHBV) with peach palm particles and found that the degradation was faster in the biocomposites due to the presence of cavities that resulted from the introduction of the fillers. These cavities allowed for larger water adsorption and greater access to microorganisms. Enhanced biodegradation was also found by other researchers with several fillers.[16–20,24–26,28–30,32,34] The hydrophilicity of the filler seems the more important characteristic that influences the biodegradability of the matrix. Additionally, the resistance to the photo-oxidative degradation is enhanced in biocomposites by the presence of lignocellulosic filler.[32–34,36–37]

As for the applications, besides the usual manufacts produced by injection molding, some papers also report the possibility to use biocomposites both in film blowing and in 3D printing.[37,38] Nevertheless, in this relevant amount of scientific literature, to our best knowledge, no paper has been published that follows the whole life of a biocomposite system from the preparation of the manufacts to the compost burial degradation. In this work, the biocomposite systems were designed for packaging applications with the aim of being reusable and at the end of the lifetime being disposed of in the organic waste. The biocomposites have been prepared in a twin-screw extruder, mixing polylactide (PLA) and WF or powder of hazelnut shell (HS). Then specimens were obtained by compression molding and characterized from a rheological and mechanical point of view. Compression molding sheets were then subjected to UV irradiation to simulate a degradation during their use. Finally, both virgin and UV-irradiated samples were buried to simulate a real composting and compare the effect of the previous treatments on the degradation in compost.

2 | EXPERIMENTAL

2.1 | Materials and preparation of the biocomposites

The materials (polymer and fillers) used in this work and their main properties are reported in Table 1.

PLA sample was provided by Nature Works (USA), WF (mainly coming from beech trees) was supplied by La.So.Le. (Percoto, Italy), and HS powder was provided by Agrindustria Tecco (Cuneo, Italy). These fillers have been used in previous papers.[14,33]

All the biocomposites were prepared in a counter-rotating, intermeshing twin-screw extruder (OMC, Saronno, Italy) with a screw diameter of 19 mm and a length-to-diameter ratio of 25. The filler contents used were 10% and 20% by weight (Table 2). The temperature

Materials	Sample codes	MFI, g/10 min	Diameter, μm
PLA 2003 D	PLA	6	–
Wood flour	WF	–	300–500
Hazelnut shell	HS	–	120–240

TABLE 1 Materials and fillers.

TABLE 2 Sample codes and composition of all the investigated samples.

Sample codes	PLA, wt%	WF, wt%	HS, wt%
PLA EXT	100	0	0
PLA/WF10	90	10	0
PLA/WF20	80	20	0
PLA/HS10	90	0	10
PLA/HS20	80	0	20

profile used for all the systems was 150–160–170–170–170–180–180°C (die) and the screw speed was 160 rpm. The pure PLA was also subjected to the same processing. To prevent the hydrothermal degradation of PLA during processing, both PLA and the fillers were dried overnight, under vacuum, at 60 and 80°C, respectively.

The specimens for all the tests were prepared by compression molding. A Carver laboratory press (USA) was used. The samples were prepared at 180°C for about 3 min at a pressure of 300 psi. Even before the preparation of the compression-molded sheets both PLA and biocomposites were dried under vacuum at 60°C overnight.

2.2 | Photo-oxidation

The PLA and the biocomposites were exposed to accelerated weathering in a QUV chamber, equipped with eight lamps UVB-313 (Q-Labs Corp., USA). The exposure cycle conditions were 8 h of UV irradiation at a temperature of 60°C followed by 4 h condensation at the temperature of 40°C (named UV-COND). To investigate the effect of the humidity during weathering, comparative tests were also carried out on the pure PLA in the QUV with the same irradiation cycle, but only under UV irradiation. Samples were monitored at different degradation intervals (12, 24, and 36 h).

2.3 | Characterization

Mechanical characterization was performed using an Instron (USA) universal testing machine, model 3365, according to ASTM D638. The elastic modulus was measured with a crosshead rate of 1 mm/min up to a deformation of 10% and after the crosshead rate was increased to 100 mm/min until breaking. At least seven specimens were tested for each sample. All the data were validated by one-way analysis of variance (ANOVA).

Rheological characterization was carried out for all the samples at 180°C using an ARES G2 (TA Instruments, New Castle, DE, USA) with a plate-plate geometry (25 mm diameter). The angular frequency range used was of 0.1–100 rad/s.

Fourier Transform Infrared Spectroscopy Attenuated Total Reflectance (ATR-FTIR) spectra were performed with a Perkin-Elmer (USA) Spectrum One spectrometer, using Spectrum software. The spectra were obtained through 8 scans with a 4 cm^{-1} resolution. Measurements were attained from the average of triplicate samples. The ATR spectra were normalized using the peak located at 2995 cm^{-1} attributed to the asymmetric stretching of CH_3 groups.[40]

SEM images were acquired by using a Phenom proX scanning electron microscope (Phenom World, Eindhoven, Netherlands). Before examination, the samples were cracked in liquid nitrogen. Analysis of SEM images was performed by ImageJ software.

Nuclear magnetic resonance experiments were conducted with an Agilent ^{UNITY}INOVA spectrometer (Santa Clara, CA, USA) working at 500 MHz (^{1}H). Spectra were recorded at 27°C in $CDCl_3$ with 0.03% TMS v/v as an internal standard and with the following Agilent acquisition parameters: sw 8012.8 Hz, at 4.089 s, d1 4 s, np 65,536, pw 45°. Spectra were processed with the MestreNova software (Mestrelab Research, Santiago de Compostela, Spain).

A contact angle goniometer (OCA15EC, Dataphysics) was employed to monitor the surface wettability of samples. Measurements were carried out at room temperature. SCA (Static contact angle) values were defined releasing 2 μL of water from a micro syringe on the surfaces. Then, the dedicated software (SCA 20) analyzed the images acquired by the connected video camera. To exclude interferences, the samples were earlier equilibrated at 40°C for 30 min and after that SCA was computed. For each sample, at least five SCA values were determined to assure repeatability of the data.

2.4 | Compost burial test

Compost burial test was performed under moisture-controlled settings and at 58.0 ± 0.1°C. Compost was provided by Biofactory S.p.A (Calcinate, BG, Italy). Triplicate specimens of the biocomposite samples were located in dark vessels arranged with a multi-layer substrate.[41] Squares of filter paper were utilized as positive controls. Biocomposite film pieces of 2 cm × 2 cm were cut. The specimens (initial weight 100–350 mg, positive control ~28 mg; PA114C Ohaus Pioneer Plus, d = 0.1 mg) were inserted between two layers of milled perlite (70 g) mixed with compost (200 g). The mixture were humidified of distilled water (100 mL). Perlite (60 g) was placed as the bottom and top layers of the multi-layer substrate and moistened with distilled water (120 mL). It was used for encouraging aeration to the compost and the retention of water. Biocomposites were unearthed after established intervals (10 and 30 days), brushed gently, cleaned with distilled water numerous times, and dried at room temperature, in the presence of P_2O_5, under vacuum to constant weight.[42] The degree of degradation was estimated by WL by the Equation (1):

$$\mathrm{WL}\,(\%) = (W_i - W_t)/W_i \times 100, \tag{1}$$

where W_i is the weight of the sample at the starting time and W_t is the weight after a fixed time.

3 | RESULTS AND DISCUSSION

3.1 | Mechanical, rheological, and morphological characterization of the biocomposites and influence of photo-oxidation

Figure 1 reports the flow curves of the PLA and of two biocomposites with two different compositions. To investigate a possible thermomechanical degradation during the extrusion, the flow curve of the unprocessed PLA is also reported. The flow curves of the two PLA samples are very near indicating that the PLA does not undergo severe degradation phenomena during processing due to the thermomechanical stress acting on the melt.

The rheological behavior of the two biocomposites is quite unusual. Indeed, usually the composites with inert fillers show a viscosity increasing with increasing the content of filler.[40] On the contrary, in these two cases, the viscosity of the biocomposites decreases in the presence of the filler, and, in particular, the biocomposite with 10% of WF filler shows a lower viscosity. The flow curve of the biocomposite with 20% of filler is higher, although still lower than that of the pure, processed matrix; moreover, the flow curves do not show the typical Newtonian plateau at low frequency, but the flow curves tend to grow up. This last behavior is typical of the polymer composites with inert filler and the upturn at low frequency suggests the presence of a yield stress. The decrease of the viscosity in presence of fillers, then, is quite unusual, as the presence of inert fillers should induce an increase of the viscosity. This behavior, however, could be explained considering both a very poor adhesion between the two phases and/or some thermomechanical degradation of the matrix during the processing.

As for the morphology of these systems, in Figure 2 the SEM micrographs of the biocomposites with a filler content of 20% are reported.

The morphology of the two samples is typical of composites with low adhesion between matrix and fillers in both cases and a broad range of dimension is observed. The morphology of both samples can certainly justify the lower viscosity of the biocomposites with respect to that of the pure matrix. However, it is not possible to interpret only based on the morphology the lower flow curves of the samples with WF (Figure 1).

As for the thermomechanical degradation during processing, although no relevant degradation of the pure PLA has been previously observed, the increase of the viscosity, due to the presence of the filler with consequent increase of the mechanical stress acting on the melt during processing, could cause some degradation. The flow curves that we measured are, indeed, the flow curves of the degraded material after the processing. During processing, the pushing force of the thermomechanical degradation is the temperature and the mechanical stress. The processing temperature is the same for both systems, while the mechanical stress is:

$$\tau = \eta * \gamma, \tag{2}$$

where η is the viscosity at the processing conditions and γ the shear rate. The typical shear rate range in extrusion operations is about 100 s^{-1} and in this shear rate range the viscosity of the filled systems is very near or even higher than that of the PLA. Some thermomechanical degradation more severe than that observed for the PLA can be considered responsible for this unusual behavior, at least in part.

The mechanical properties, elastic modulus, E, tensile strength, TS, and elongation at break, EB, are reported in Table 3 for all the investigated samples. As expected, the elastic modulus increases in presence of the filler and with increasing the filler content ($p < 0.05$). On the contrary, tensile strength and elongation at break decrease

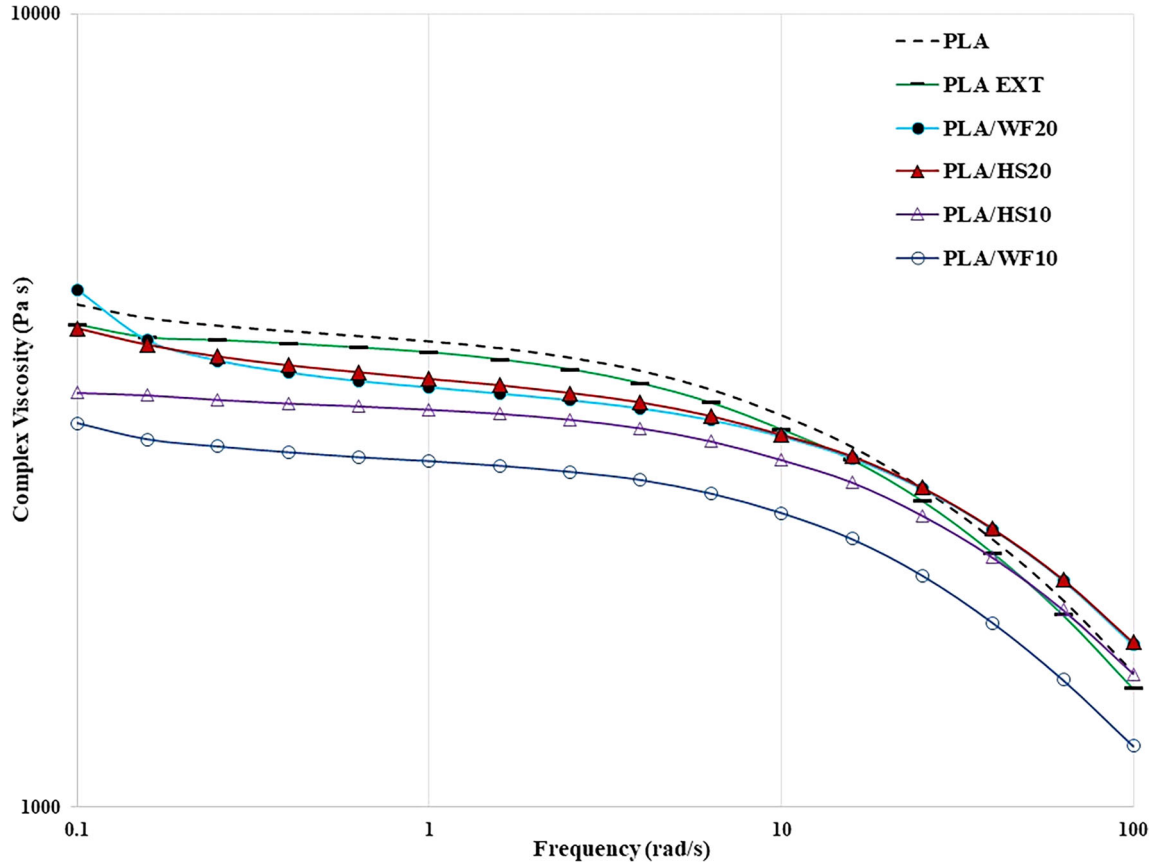

FIGURE 1 Flow curves of PLA and of the two biocomposite systems.

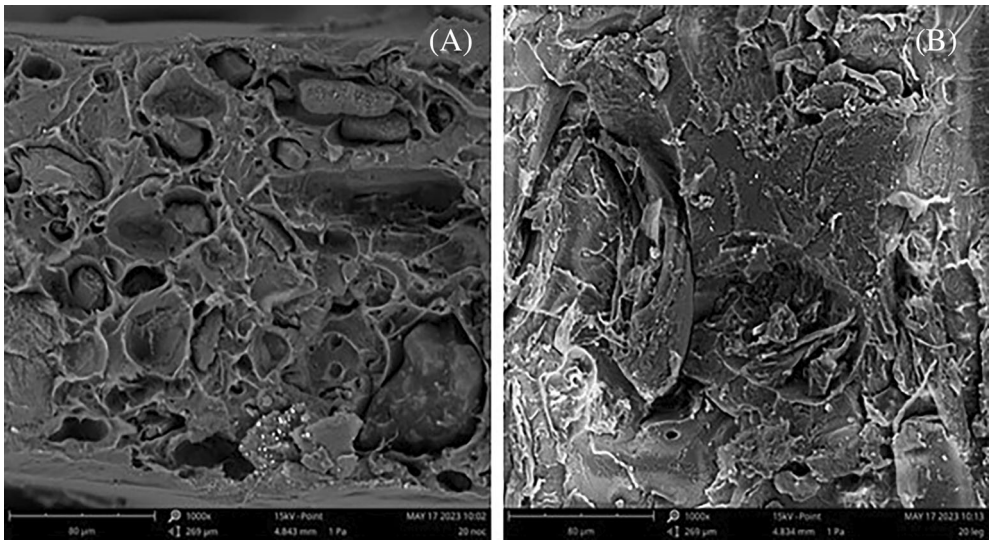

FIGURE 2 SEM micrographs of biocomposites with 20% of (A) HS and (B) WF.

with increasing the filler content ($p < 0.05$). The presence of an inert filler increases the rigidity of the PLA and reduces its deformability. The reduction of the deformability also causes a decrease of the tensile strength for the premature breaking of the sample. It is worth to mention that the reproducibility of the experimental data is good for all the biocomposites. This means that, in all the systems, the filler particles are quite well dispersed. The biocomposite with WF shows slightly better properties, in particular a higher tensile strength.

In Figure 3, the flow curves of the PLA and all the virgin biocomposites, photo-oxidized for 36 h (with and

TABLE 3 Mechanical properties of PLA and of the biocomposites.

Materials	E (MPa)	TS (MPa)	EB (%)
PLA	1540 ± 51*	38.3 ± 6.9*	4.0 ± 0.63*
PLA/HS10	1572 ± 88*	24.3 ± 2.0*	2.3 ± 0.22*
PLA/HS20	1674 ± 74*	21.4 ± 1.7*	1.5 ± 0.18*
PLA/WF10	1567 ± 19*	27.5 ± 1.5*	2.5 ± 0.13*
PLA/WF20	1690 ± 64*	24.0 ± 1.8*	1.9 ± 0.3*

*Significant at $p \leq 0.05$.

without condensation cycle) and not, are reported. The flow curves of the PLA and of the biocomposites, weathered 36 h, are lower than that of the virgin samples with a decrease that is more evident for the samples photo-oxidized with condensation cycles. These results clearly indicate that the samples weathered in presence of condensation cycles undergo a more relevant chain scission of the PLA. The decrease of the viscosity is almost similar for both systems. It is interesting to notice the presence of an upturn in the photo-oxidized samples at low values of

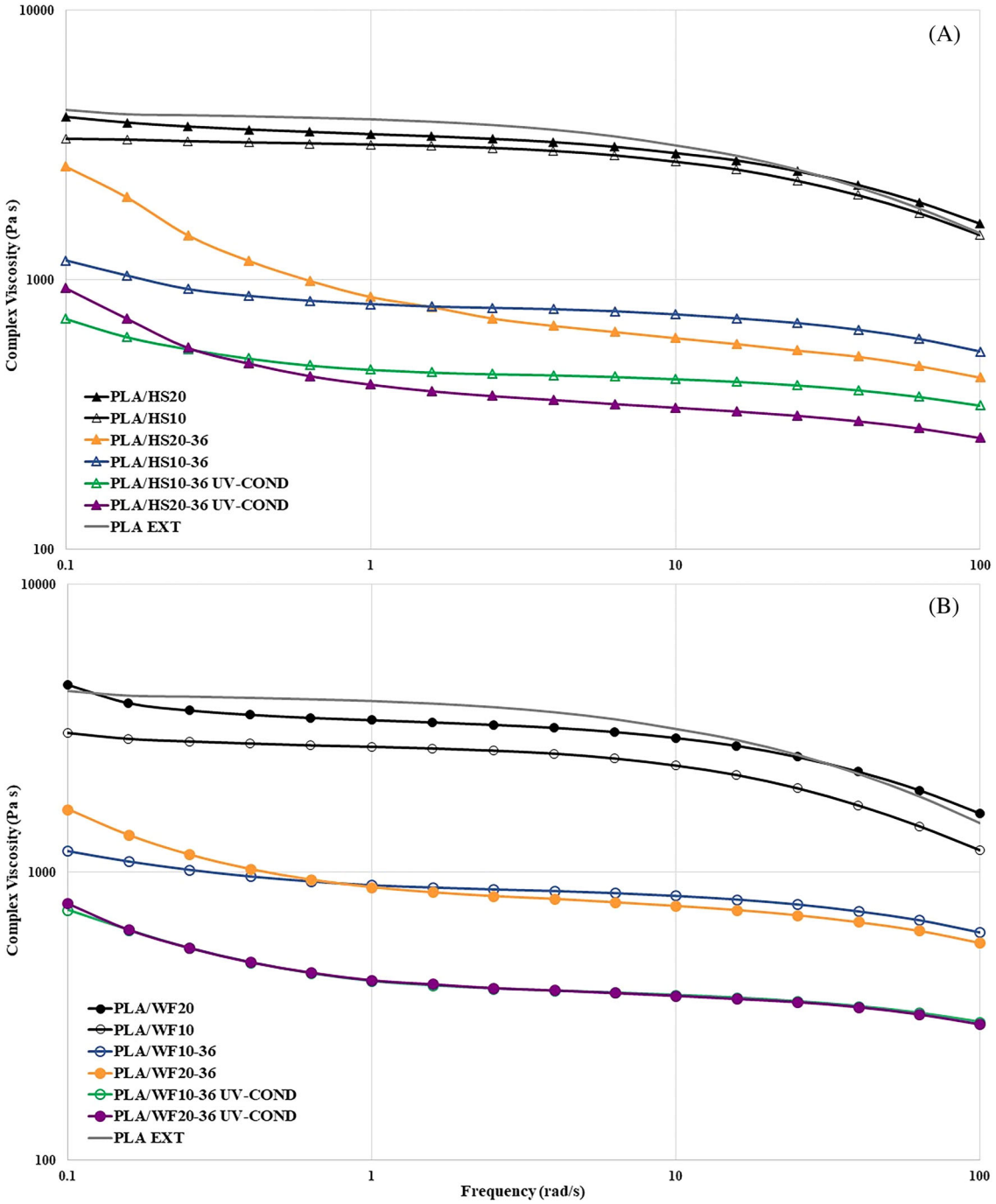

FIGURE 3 Flow curves of virgin and photo-oxidized samples: (A) PLA with HS (B) PLA with WF.

the frequency that, then, implies the apparence of a yield stress. This behavior is to attribute to the presence of inert fillers. The apparence of the yield stress at these frequencies—not present in the virgin sample—is certainly due to the reduction of the viscosity of the matrix and to the more relevant influence of the inert filler during the flow with respect to the higher viscosity virgin sample.

However, the more severe photo-oxidative degradation is observed for the PLA matrix (Figure 4) where the flow curves of the PLA samples aged under photo-oxidation for 36 h and under a cycle with both UV irradiation and condensation are reported. The flow curves of the PLA aged only under UV irradiation is much higher than that of the same polymer aged under a cycle with UV irradiation and condensation. Consequently, the macroscopic effects measured on this last sample are due mainly to the hydrolytic degradation that gives rise to chain scission and not to the oxidation. The effect of the hydrolytic degradation is very effective as the viscosity decreases of more one decade after this relatively short treatment. In fact, noteworthy, under the weathering carried out with a cycle involving 4 h of condensation, the decrease of the flow curves for the biocomposites is much lower than that induced in PLA. This result could be due to the protective action of the lignin, which is a component of both WF and HS during the photo-oxidation[15] but it could be related to a hydrolytic stabilization outcome induced by the fillers as well. This effect could be very relevant for a PLA-based packaging aimed to be reusable.

The decrease of the viscosity is reasonably due to the reduction of the weight average molecular weight (Mw) because the Newtonian viscosity is strongly dependent on the Mw according to the equation:

$$\eta_0 = \mathrm{kMw}^{3.4}, \tag{3}$$

where k is a constant. The dimensionless molecular weight, $\overline{Mw}$, for each sample can be evaluated as:

$$\overline{Mw} = (\eta_0(t)/\eta_0(0))^{1/3.4}, \tag{4}$$

where $\eta_0(t)$ is the value of the Newtonian viscosity of the samples photo-oxidized 36 h and $\eta_0(0)$ the Newtonian value of the same virgin sample. Considering the previous equations, the decrease of the molecular weight for PLA under UV photo-oxidation is only about 20% while

TABLE 4 Dimensionless viscosity for all the investigated samples weathered 36 h.

Samples	$\eta(t)/\eta(0)$	$\overline{\mathrm{Mw}}$
PLA	0.06	0.43
PLA/HS10	0.15	0.58
PLA/HS20	0.12	0.54
PLA/WF10	0.16	0.58
PLA/WF20	0.11	0.52

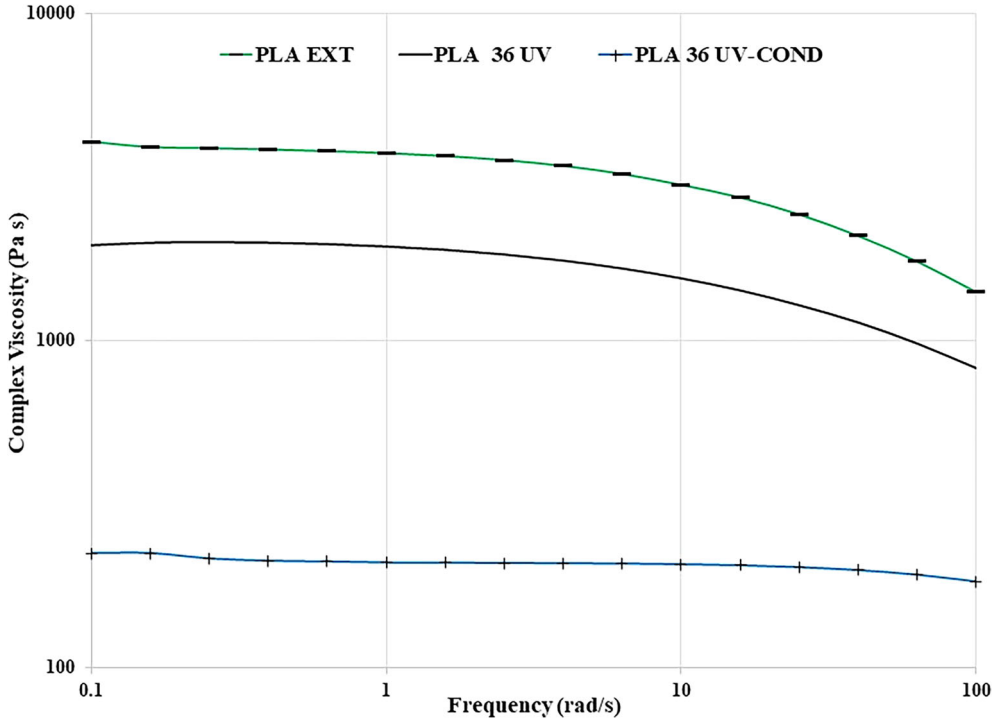

FIGURE 4 Flow curves of the extruded PLA and of the same sample degraded under UV irradiation and under UV irradiation and condensation.

the reduction of the molecular weight for the sample aged under condensation and UV cycle is about 60% (Figure 4).

Of course, these equations hold for homogeneous polymer systems, but it is reasonable consider that only the decrease of the molecular weight of the matrix is the cause of the decrease of the viscosity because the adhesion between matrix and filler and the dimensions and shape of the filler do not change with the processing. The value of the Newtonian viscosity for the biocomposites cannot be evaluated from the flow curves of Figure 3 because of the presence of an upturn in the low frequency range, for this reason Equation (4) could not be applied. However, we can use the viscosity values in the flat zone and evaluate the ratio of the viscosity as an indicator of the decrease of the molecular weight. The values of the dimensionless viscosity, calculated as:

$$\eta(t)/\eta(0), \tag{5}$$

at a shear rate of 1 s^{-1} are reported in Table 4. At this shear rate, the flow curve of the PLA matrix is still in the Newtonian zone.

TABLE 5 Mechanical properties of photo-oxidized PLA and biocomposites.

Materials	E (MPa)	TS (MPa)	EB (%)
PLA-36	-	-	-
PLA/HS10-36 UV-COND	1518 ± 96 (n.s.)	21.4 ± 2*	1.9 ± 0.1*
PLA/HS20-36 UV-COND	1517 ± 87 (n.s.)	18.8 ± 2.8*	1.6 ± 0.4*
PLA/WF10-36 UV-COND	1571 ± 113 (n.s.)	24.8 ± 2.9*	2.1 ± 0.2*
PLA/WF20-36 UV-COND	1596 ± 117 (n.s.)	21.9 ± 2.7*	1.9 ± 0.4*

Abbreviation: n.s., not significant.
*Significant at $p \leq 0.05$.

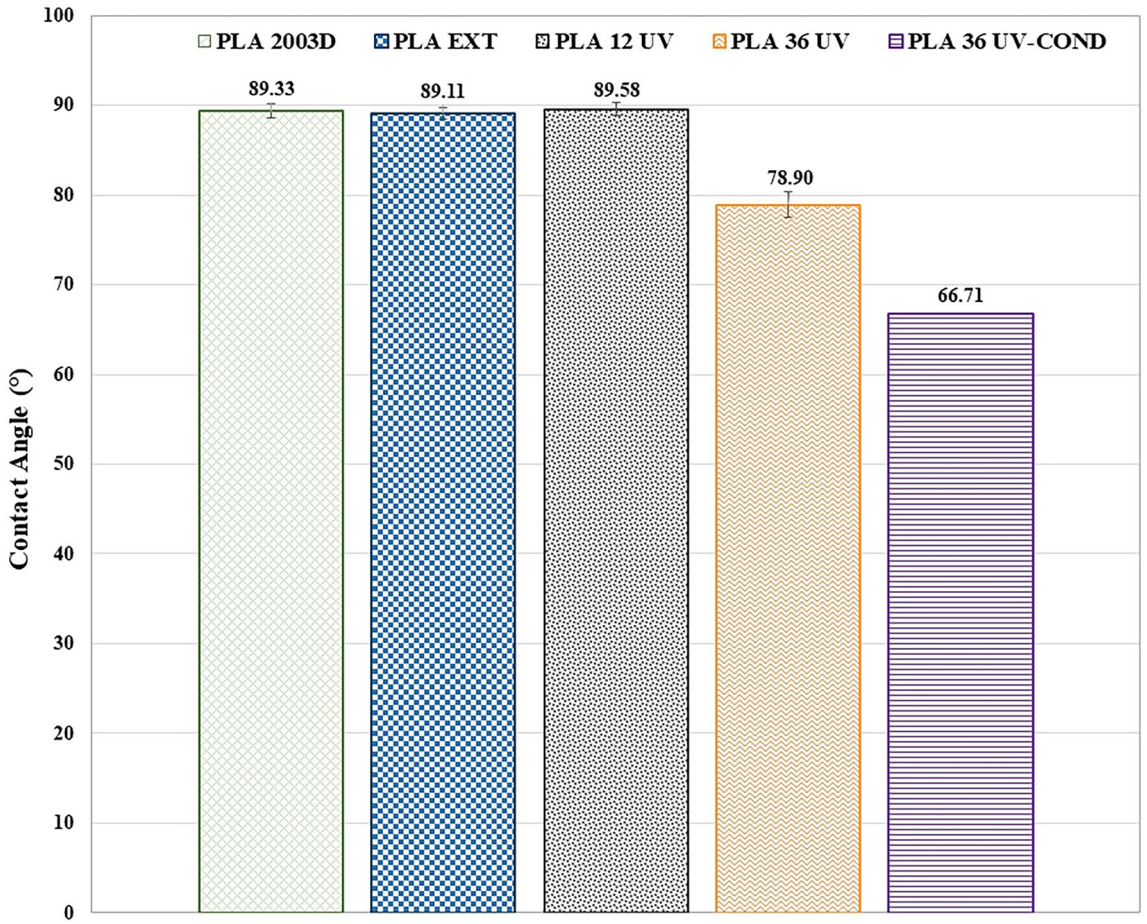

FIGURE 5 Average static contact angle values for the PLA film samples virgin and photo-oxidized under different conditions.

Although, as said before, it should not be possible to use Equation (4) because the Newtonian plateau is not observed for some samples, we have used this equation to obtain a rough evaluation of the reduction of the molecular weight because the viscosity at 1 s^{-1} is in the Newtonian plateau of almost all the samples. The reduction of the molecular weight is much higher for the pure PLA and lower for the two biocomposites confirming the dramatic chain scission undergone by the PLA during photo-oxidation and an UV-stabilization effect induced by the fillers. As reported before, the effect of the weathering is similar for both fillers and only very slightly higher for the PLA/WF biocomposite.

The mechanical properties of the photo-oxidized samples are reported in Table 5 for all the investigated samples. For the weathered PLA sample, it was not possible to carry out the mechanical test because the sample becomes too brittle after 36 h of photo-oxidation. This result would seem to confirm once again the protective effect by the two fillers that involves less severe photo-oxidative degradation of the PLA matrix ($p < 0.05$).

3.2 | Chemical–physical and structure modifications induced by fillers and photo-oxidation

The hydrophilicity/hydrophobicity of a surface has a relevant impact on the hydrolysis and biodegradation rate. A greater hydrophilicity implies a higher water adsorption capability that provides a larger hydrolysis rate.[43] Accordingly, the wettability of the biocomposite samples, before and after accelerated photo-oxidation, was monitored by using SCA analysis. Figure 5 shows that the SCA values of PLA noticeably decreased after 36 h of photo-oxidation, due to the new hydrophilic chain ends originated. Chemical changes, stimulated by oxygen and light, on the surface of the films, enhanced the wettability of PLA samples, underlined by the decrease of SCA values. The wettability increase was more pronounced after the weathering with a condensation cycle. On the contrary, the presence of WF and HS fillers affected the changes of SCA values induced by photo-oxidation (Figure 6) suggesting again a UV light stabilization effect. In fact, SCA values are unchanged or increased after 36 h of photo-oxidation and the increase in surface wettability induced

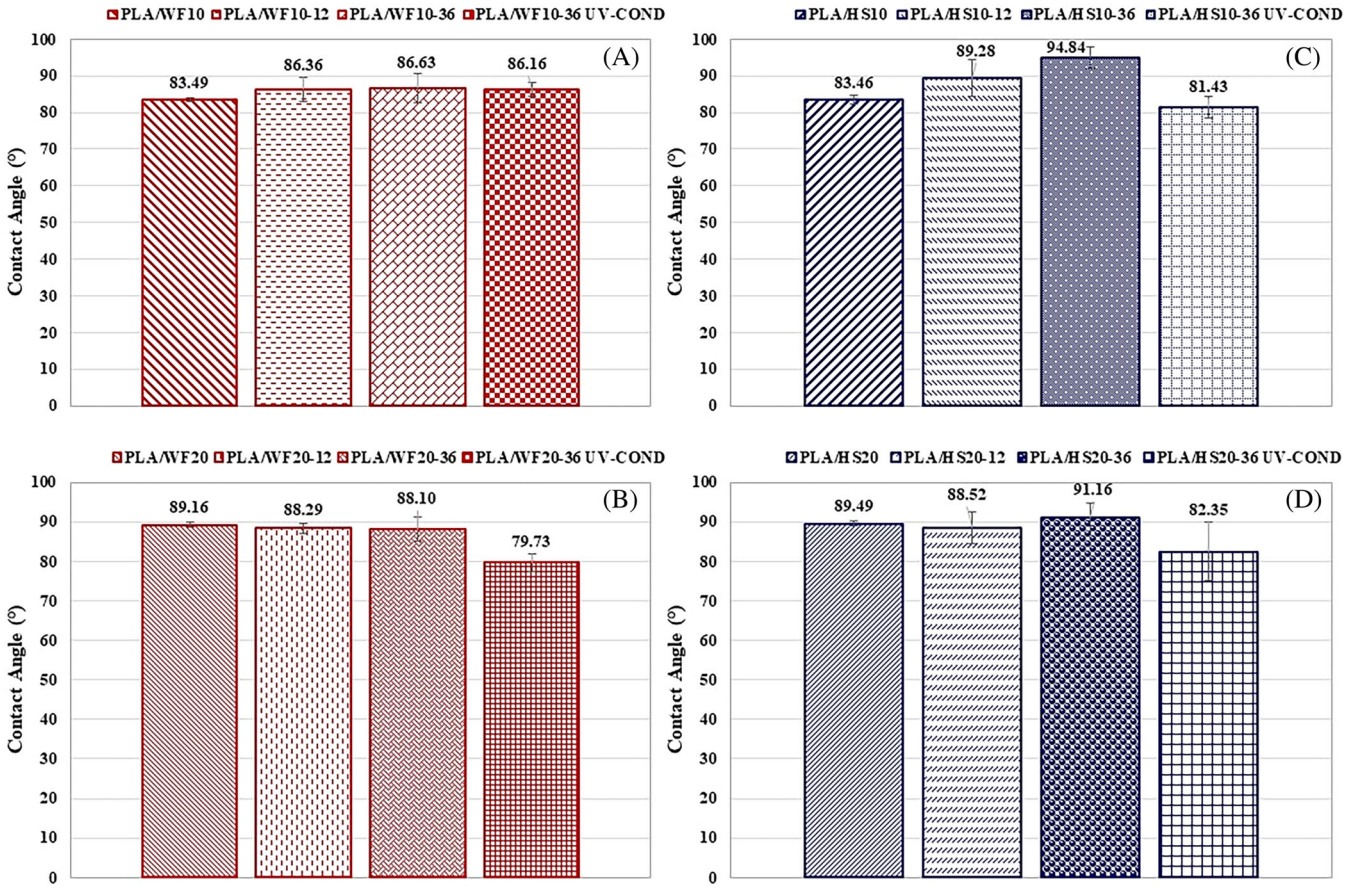

FIGURE 6 Average static contact angle values for the PLA nanocomposite films with (a, b) WF (10% and 20%) and (c, d) HS (10% and 20%), virgin and photo-oxidized under different conditions.

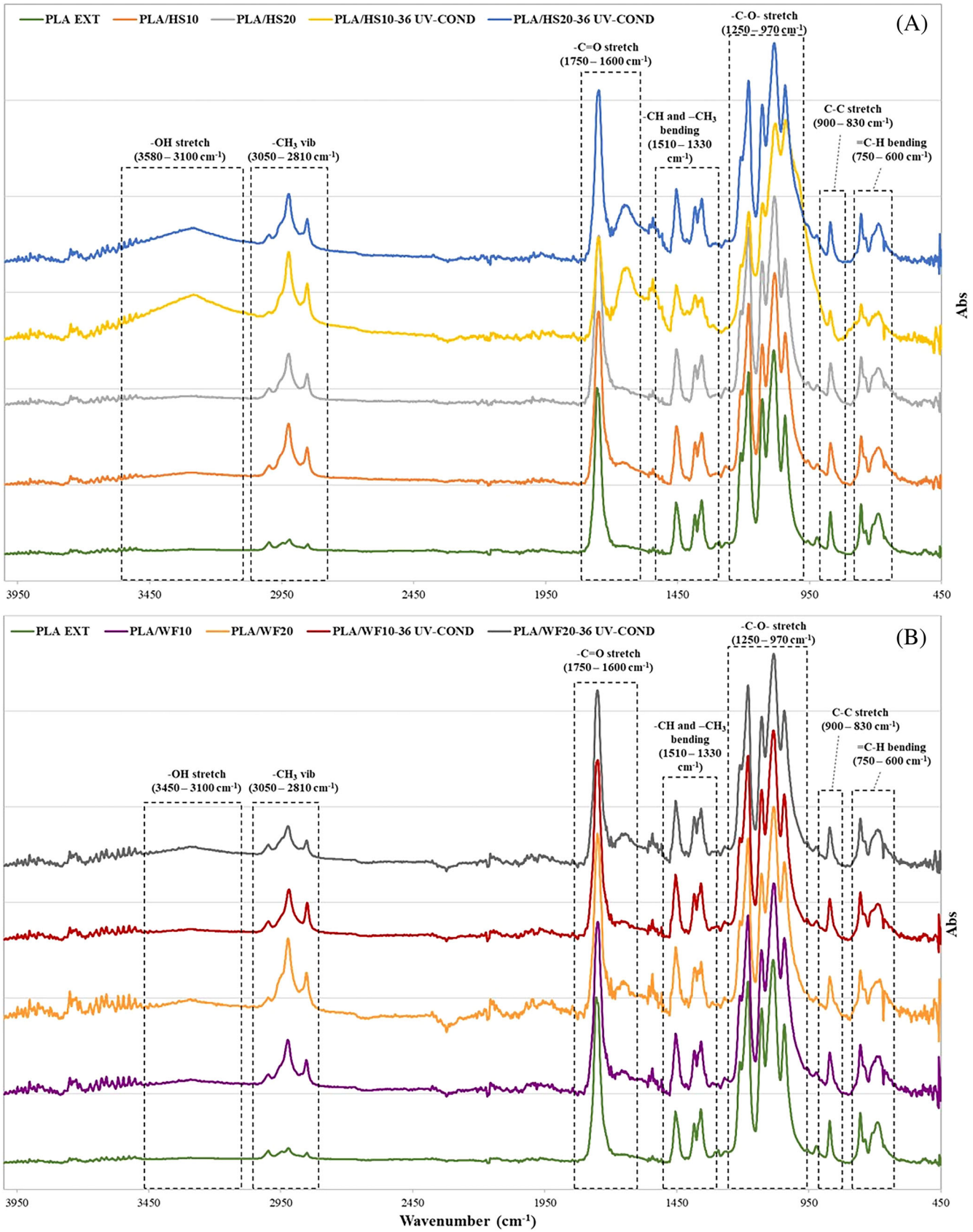

FIGURE 7 ATR-FTIR spectra of (A) PLA/HS and (B) PLA/WF biocomposites photo-oxidized 36 h +condensation cycle.

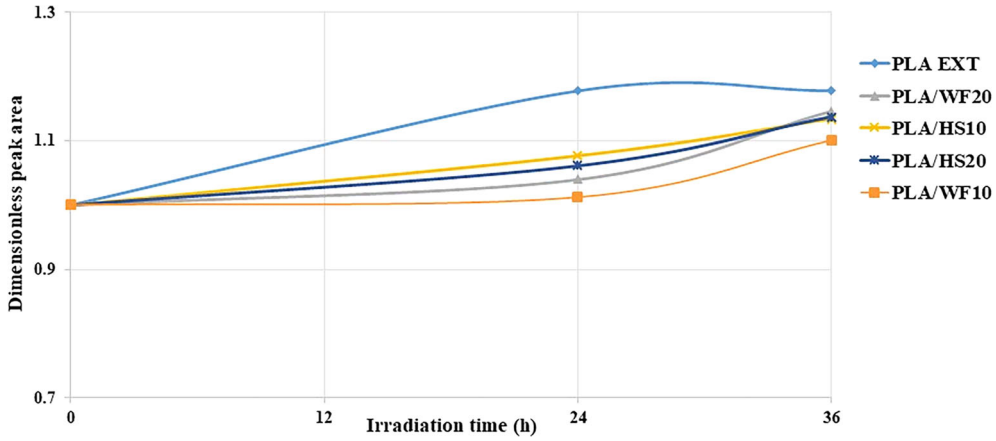

FIGURE 8 Dimensionless area under the 1600–1830 cm^{-1} as a function of UV irradiation time. With condensation cycle.

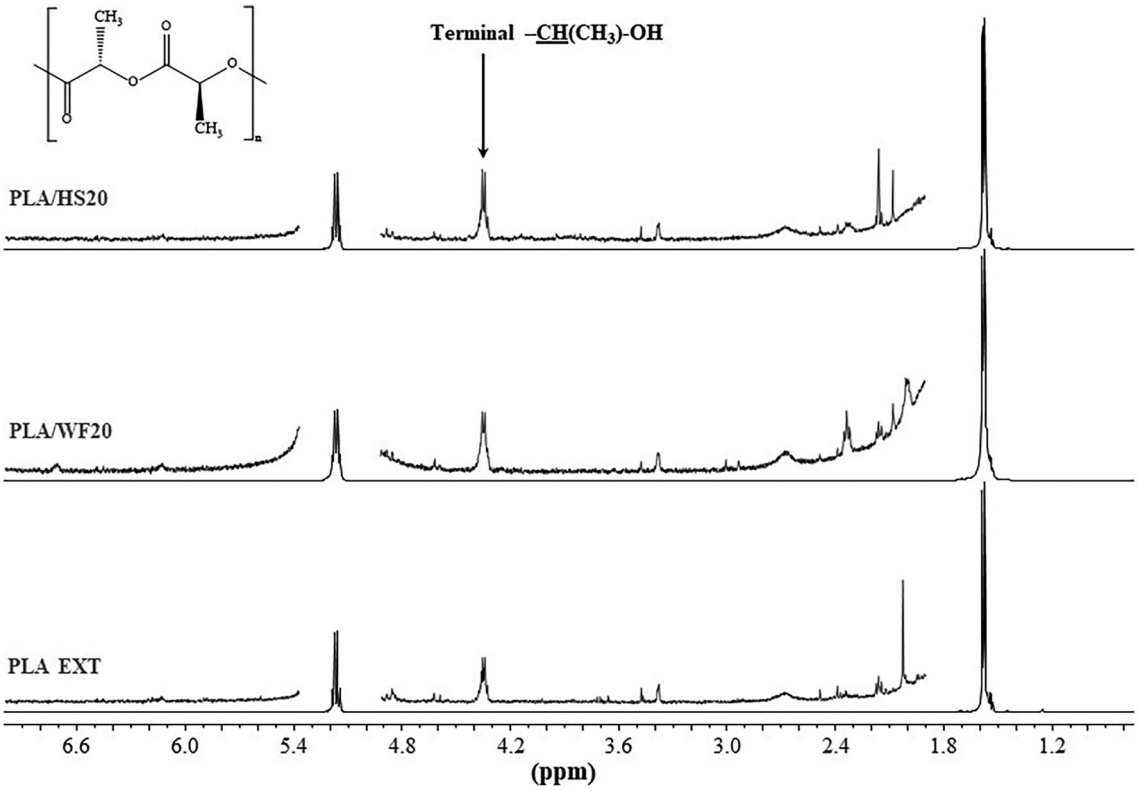

FIGURE 9 ^{1}H NMR spectra of PLA extruded and PLA loaded with 20% w/w WF and HS.

by weathering with a condensation cycle was less pronounced for the biocomposites (Figure 6, ΔCA ~2–10°) than for the PLA (Figure 5, ΔCA ~10–22°).

In Figure 7, the ATR-FTIR spectra of PLA and biocomposites, virgin and photo-oxidized (UV + condensation cycle) samples, are reported for the two systems. PLA can be distinguished by the presence of signals associated to the —CH_3 groups at 1510–1330 cm^{-1}, corresponding respectively to the out-of-phase bending (δ_{as}) and in-phase bending (δ_s), and at 3050–2810 cm^{-1}, related to the asymmetric (ν_{as}) and symmetric (ν_s) stretching. The most intense peaks, at 1750 cm^{-1} and 1250–970 cm^{-1}, are respectively associated to the C═O ($\nu_{C=O}$) and the C—O ($\nu_{C—O}$) groups stretching.[44] For all samples, compared to the extruded PLA, an increase in the absorption peaks is observed in the regions relating to the CH_3 vibrational and the C—O stretching. In agreement with a hydrolytic process, the bands relating to the carboxyl acid carbonyl C═O and —OH increase in the photo-oxidized samples, and this effect is more pronounced in PLA/HS (Figure 7A) than in PLA/WF (Figure 7B). The signal relating to the ester carbonyl C═O decreases in the case of composite samples subjected to photo-oxidation, while a measurable increase of the absorbance of the peak centered around 1650 cm^{-1} is

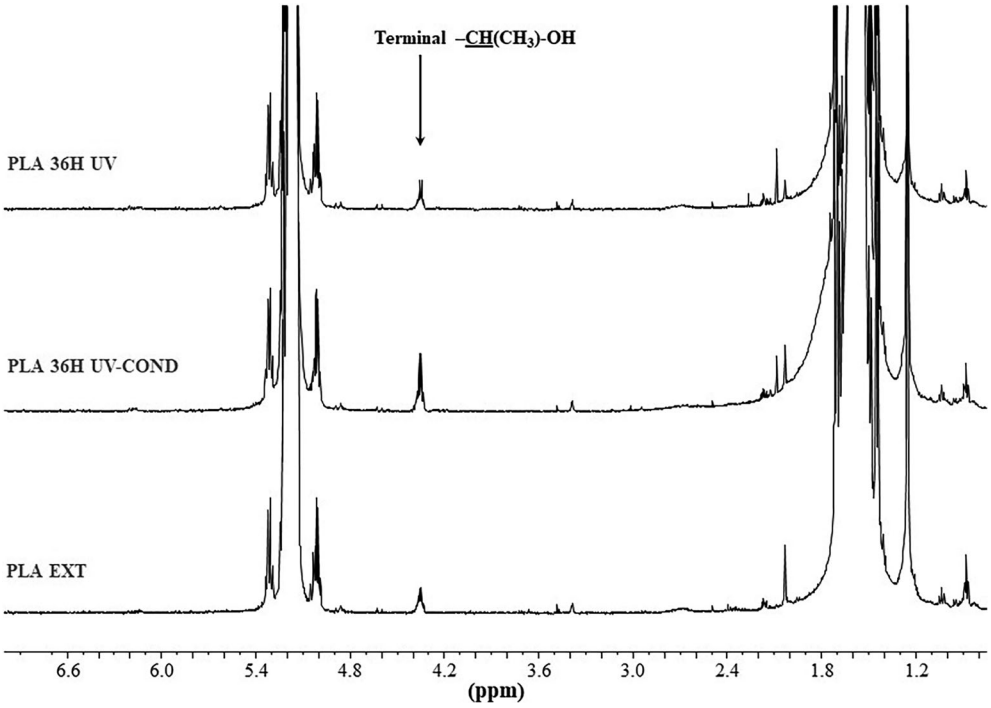

FIGURE 10 ^{1}H NMR spectra of extruded PLA (PLA EXT), PLA subjected to UV weathering with (PLA 36 h UV-COND) and without (PLA 36 h UV) condensation cycle.

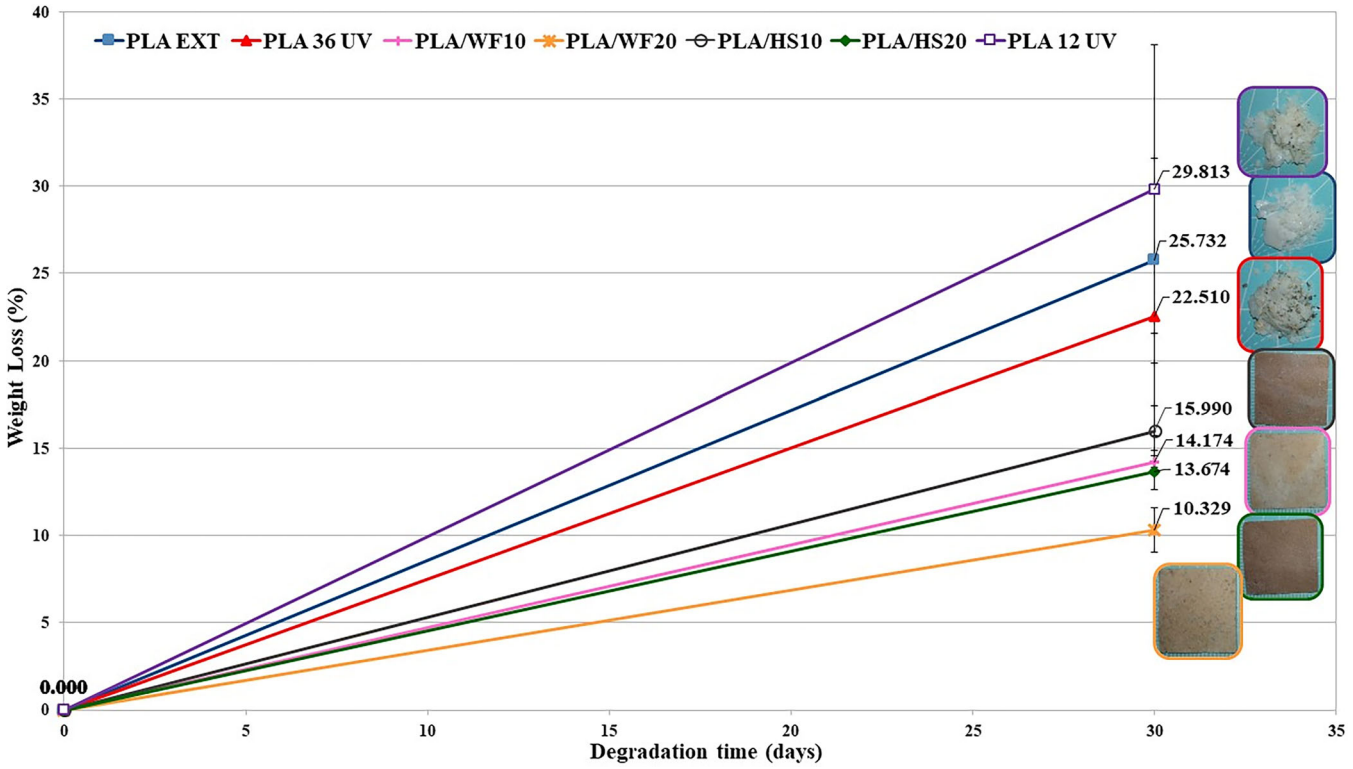

FIGURE 11 Average weight losses versus degradation time at 58°C for PLA and biocomposite samples.

observed, not present in the spectra of PLA EXT sample, and characteristic of the stretch of carbonyl of carboxylic groups.[45]

In biocomposites, the peak at 1746 cm^{-1}, attributed to the ester groups, is slightly decreasing, but at the same time, the area under the wavelength range 1600–1830 cm^{-1} is slightly increasing as reported in Figure 8. In this figure, the dimensionless area under the peak at 1600–1830 cm^{-1} are reported as a function of the photo-oxidation time for all samples. The area under this peak

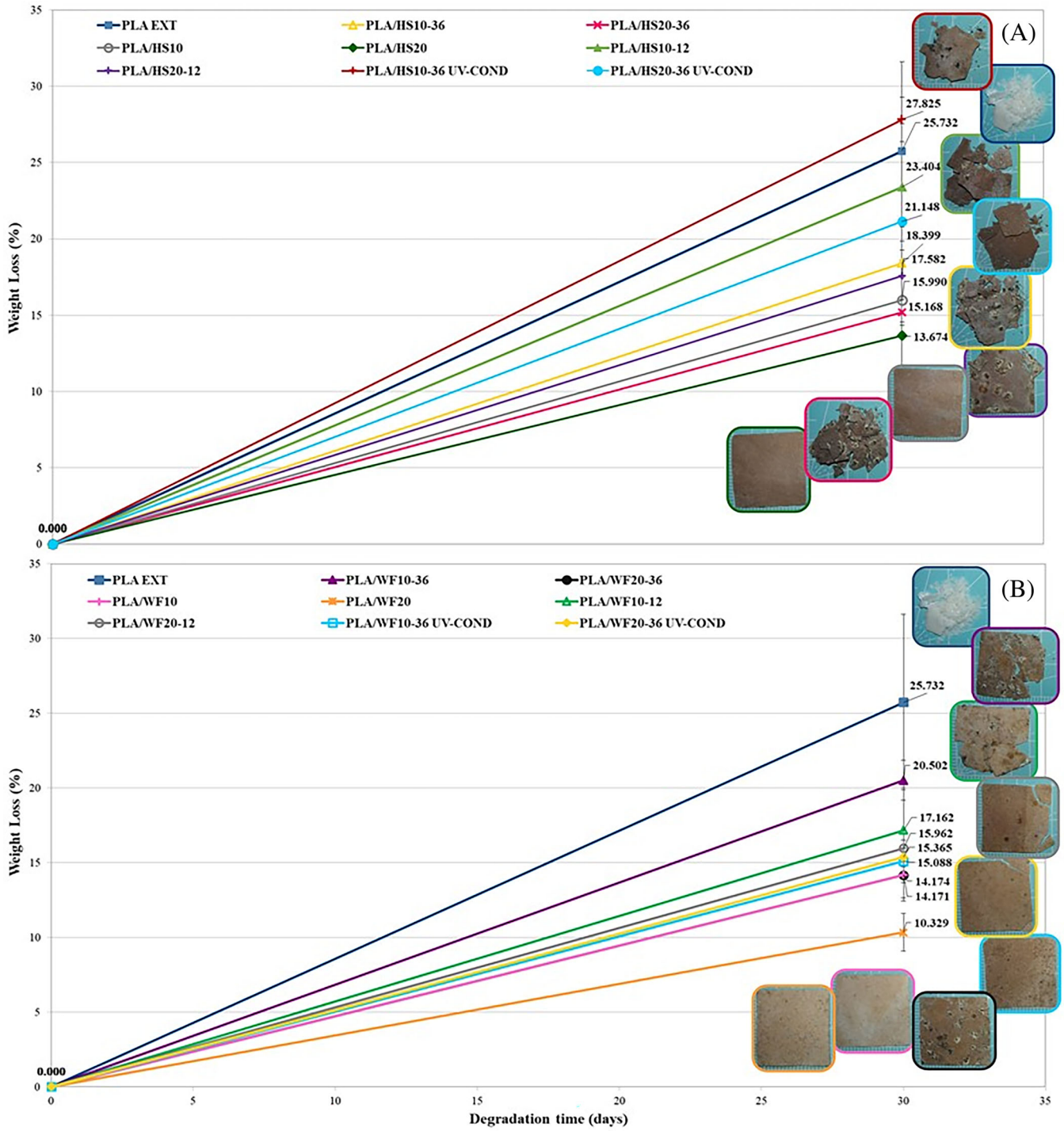

FIGURE 12 Average weight losses versus degradation time at 58°C for PLA biocomposite samples (A) with HS (10% and 20%) and (B) WF (10% and 20%) fillers, photo-oxidized and not.

represents the concentration of all the C═O groups present in the macromolecular chains.

The curve relative to the matrix indicates a slight increase, about 15%, of the area relative to all the C═O groups. This could be explained by hypothesizing that the photo-oxidation contribute to the formation of other types of carbonyl groups as already reported in a previous paper for PLA.[40] Similar comments can be made for the biocomposites. However, in this case, the change of area is much more slow and still less pronounced confirming the protective effect of the lignin contained in the fillers. The WF filler seems to be slightly more effective than HS in protecting the PLA matrix against the photo-oxidation. No peak at 1845 cm^{-1} of the anhydrides, typical

functional groups found in the photo-oxidation of PLA,[40] has been observed in all the samples. Thus, it is evident that the oxidation of the PLA matrix is very small and certainly does not compatible with the dramatic decrease of the viscosity and of the molecular weight which in fact has been attributed mainly to hydrolytic scission. It is then clear that the decrease of the molecular weight is not accompanied by a formation of other oxygenated species.

Samples were also investigated by NMR to gain information on the terminal groups originated from the chain scission reactions leading to the reduction of MW illustrated in the preceding paragraphs. The ^{1}H NMR spectra of PLA extruded, and PLA loaded with 20% w/w WF and HS are shown in Figure 9. The polymer repeating unit methyl and methine protons give rise to a doublet at 1.57 ppm and a quartet at 5.17 ppm, respectively.[44] A vertical magnification of the spectra shows that, besides the main signals of the PLA repeating unit, there is a small resonance at 4.35 ppm that is assigned to the terminal lactic acid unit bearing a free hydroxyl group, which constitute the main termination of the polymer. The similar intensity of this peak in these samples indicates that there is no or very little depolymerization during the extrusion of PLA with WF or HS.

In Figure 10 the proton spectra of extruded PLA (PLA EXT), PLA subjected to UV weathering with and without condensation (PLA 36H UV-COND and PLA 36H UV) are shown. The resonance at 4.35 ppm, a proof of hydrolytic depolymerization, is clearly more intense in the sample subjected to UV irradiation with condensation. Photo-oxidative chain scission is absent or negligible, as these reactions lead to formation of terminal groups resonating at lower magnetic field, usually between 7 and 5 ppm.[44] Therefore, NMR data confirm the conclusion deduced from FTIR spectra.

3.3 | Compost burial degradation

The biodegradation process can be outlined in three-steps. At first, external the microbial cell, polymer chains are cut into monomers and oligomers; successively, the low molecular weight products pass through the microbial cell wall, and in the final step they are metabolized, using O_2 and releasing CO_2 and H_2O (under aerobic conditions). Almost all standardized methods, focused on the determination of biodegradation degree, are based on the analysis of the conversion into CO_2 of the organic carbon originally existent in the polymeric material (e.g., ISO 19679:2020, ISO 17556:2019, ISO 14855-1:2012, ISO 14855-2:2018). Conversely, in the literature, most of the papers regarding biodegradation of polymers, blends, or composites use WL checking, which is recognized as an index of biodegradability of plastic films.[5,46–47] Additionally, the laboratory procedures based on WL measurements are more similar to the degradation tests carried out in the open environment.

In Figures 11 and 12, the average WLs reported versus the compost burial degradation time of PLA photo-oxidized with or without condensation cycle are shown, together with those of the biocomposite samples, with 10% and 20% of fillers. A representative photographic documentation is shown for each type of film sample, recovered after 30 days of degradation in compost. PLA samples (virgin, photo-oxidized 12 and 36 h) were all brittle and the degradation in compost generated several plastic fragments and WL values with high standard deviations. Both fillers induced a high resistance and lower WL percentages (Figure 12). In agreement with our previous studies,[48–50] photo-oxidation increased the WL in both type of biocomposites with increasing weathering time exposure and with the condensation cycle (Figure S1).

4 | CONCLUSIONS

To reduce the environmental impact of plastics, biocomposites are an important tool produced by loading a biodegradable matrix with organic fillers. Biocomposites are, then, biodegradable and, depending on the matrix, compostable. In this work, sustainable and degradable biocomposites were prepared using a bio-based and compostable PLA and biowaste-derived fillers. PLA based biocomposite systems were formulated in a twin-screw extruder with 10% and 20% of WF and HS fillers. Compression molding specimens of PLA and biocomposites were then subjected to UV irradiation to simulate a severe degradation during their lifetime. To test their processability and mechanical performance, the rheological and mechanical properties of the materials were investigated and studied in comparison with those of the virgin polymer, assessing the influence of photo-oxidation. Usually, the presence of inert fillers in a polymeric matrix increases the viscosity of the composite and this means, in many cases, a worsening of the processability. In our instance, the flow curves of the biocomposite samples are, on the contrary, lower than that of the virgin PLA matrix. In particular, the biocomposite with WF shows the lower viscosity. This behavior has been attributed to the strong incompatibility between the matrix and the two inert fillers with consequent very poor adhesion and slipping between the two phases. Moreover, a more severe thermomechanical degradation with a reduction of the molecular weight in the biocomposite with respect to the degradation of the matrix could also contribute to

this behavior. Additionally, the very poor adhesion between the two phases could be considered also responsible for the decrease of the tensile strength and elongation at break. However, it is worth to notice that the elongation at break is lower also for the brittle PLA matrix. A slight increase of the modulus is observed, in particular, for the biocomposite with the WF.

The effect of photo-oxidation by UV-irradiation and the combined influence of humidity was studied as well. The employment of bio-wastes resulted in biocomposites with increased UV resistance and lower degradation rate in compost, as demonstrated by mechanical and chemical–physical analyses and burial degradation test in compost. The presence of the lignin of the fillers—a stabilizer against the photo-oxidation – is responsible for this behavior.

Both virgin and UV-degraded samples were buried to simulate a real composting and to compare the effect of the fillers and UV irradiation on the degradation in compost. Both fillers induced a high resistance to degradation in compost. However, degradation rate in compost increased in both type of biocomposites with the photo-oxidation. Overall, the experimental data showed improved mechanical properties and enhanced UV resistance of the PLA as well as a reduced susceptibility to compost degradation of the biobased biocomposites, with a WL in 30 days up to ca. 25% for PLA and 10%–15% for the biocomposites. Predictably, photo-oxidation increased the WL in both type of biocomposites with increasing weathering time exposure and with the condensation cycle.

ACKNOWLEDGMENTS

This research was partially financially supported by Sicilian Region PO FESR 2014–2020. Action 1.1.5, project "New therapeutic strategies in ophthalmology: bacterial, viral and microbial infections – NUSTEO", CUP: G68I18000700007 – application code 08CT2120090065. Biofactory S.p.A (Calcinate, BG, Italy) is gratefully acknowledged for supplying the compost for degradation tests. Many thanks are due to Roberto Rapisardi (CNR IPCB Catania, Italy) for skilled technical assistance.

CONFLICT OF INTEREST STATEMENT

The authors declare that they have no conflicts of interest to this work, and do not have any commercial or associative interest that represents a conflict of interest in connection with the work.

DATA AVAILABILITY STATEMENT

Data will be made available on request from the authors.

ORCID

Paola Rizzarelli https://orcid.org/0000-0002-6727-4335

REFERENCES

1. John MJ. Environmental degradation in biocomposites. In: Ray D, ed. *Biocomposites for Higher Performance Applications*. Woodhead Publishing; 2017:181-194. doi:10.1016/C2015-0-04020-5
2. Shaker K, Nawaby Y, Jabbar M. Biocomposites: eco-friendly substitute of glass fibers composites. In: Kharissova OU, Torres-Martinez LM, Kharisov BI, eds. *Handbook of Nanomaterials and Nano Composites for Emerging and Environmental Applications*. Springer, Cham; 2020:1-25. doi:10.1007/978-3-030-11155-7_108-1
3. Moreira JB, Kuntzler SG, Vaz BDS, da Silva CK, Costa JAV, de Morais MG. Polyhydroxybutyrate (PHB)-based blends and composites. In: Rangappa SM, Parameswaranpillai J, Siengchin S, Ramesh M, eds. Composites Science and Engineering, Biodegradable Polymers, Blends and Composites*Biodegradable Polymers, Blends and Composites*. Woodhead Publishing; 2022:389-413. doi:10.1016/B978-0-12-823791-5.00007-7
4. Moreira JB, Kuntzler SG, da Silva CK, Costa JAV, de Morais MG. Degradation effects on the mechanical and thermal properties of the bio-composites due to accelerated weathering. In: Muthukumar C, Krishnasamy S, Thiagamani SMK, Siengchin S, eds. *Aging Effects on Natural Fiber-Reinforced Polymer Composites. Composites Science and Technology*. Springer; 2022:159-172. doi:10.1007/978-981-16-8360-2_9
5. Rizzarelli P, Degli Innocenti F, Valenti G, Rapisarda M. Biodegradation of green polymer composites: laboratory procedures and standard test methods. In: Al-Ahmed A, Inamuddin, eds. *Advanced Applications of Bio-Degradable Green Composites*. Materials Research Forum LLC; 2020:1-44. doi:10.21741/9781644900659-1
6. Soroudi A, Jakubowicz I. Recycling of bioplastics, their blends and biocomposites: a review. *Eur Polym J*. 2013;49(10):2839-2858. doi:10.1016/j.eurpolymj.2013.07.025
7. George A, Sanjay MR, Parameswaranpillai J, Siengchin S. A comprehensive review on chemical properties and applications of biopolymers and their composites. *Int J Biol Macromol*. 2020;154:329-338. doi:10.1016/j.ijbiomac.2020.03.120
8. Chang BP, Mohanty AK, Misra M. Studies on durability of sustainable biobased composites: a review. *RSC Adv*. 2020;10:17955-17999. doi:10.1039/C9RA09554C
9. Gonzalez-Lopez ME, Martín del Campo AS, Robledo-Ortíz JR, Arellano M, Perez-Fonseca AA. Accelerated weathering of poly(lactic acid) and its biocomposites: a review. *Polym Degrad Stab*. 2020;179:109290. doi:10.1016/j.polymdegradstab.2020.109290
10. Sobczak L, Lang RW, Haider A. Polypropylene composites with natural fibers and wood – general mechanical property profiles. *Compos Sci Technol*. 2012;72(5):550-557. doi:10.1016/j.compscitech.2011.12.013
11. Sasimowski E, Majewski L, Grochowicz M. Analysis of selected properties of biocomposites based on polyethylene with a natural origin filler. *Materials*. 2020;13(18):4182. doi:10.3390/ma13184182
12. Elkhouly HI, Rushdi MA, Abdel-Magied K. Eco-friendly date-seed nanofillers for polyethylene terephthalate composite reinforcement. *Mater Res Express*. 2020;7(2):025101. doi:10.1088/2053-1591/ab6daa

13. Oulidi U, Nakkabi A, Elaraaj I, Fahim M, El Moualij N. Incorporation of olive pomace as a natural filler in to the PA6 matrix: effect on the structure and thermal properties of synthetic polyamide 6. *Chem Eng J Adv*. 2022;12:100399. doi:10.1016/j.ceja.2022.100399
14. La Mantia FP, Morreale M. Accelerated weathering of polypropylene/wood flour composites. *Polym Degrad Stab*. 2008;93:1252-1258. doi:10.1016/j.polymdegradstab.2008.04.006
15. Averous L, Boquillon N. Biocomposites based on plasticized starch: thermal and mechanical behaviours. *Carbohydr Polym*. 2004;56:111-122. doi:10.1016/j.carbpol.2003.11.015
16. Kim H-S, Yang H-S, Kim H-J. Biodegradability and mechanical properties of Agro-flour– filled polybutylene succinate biocomposites. *Appl Polym Sci*. 2005;97:1513-1521. doi:10.1002/app.21905
17. Ibrahim MIJ, Sapuan SM, Zainudin ES, Zuhri MYM. Potential of using multiscale corn husk fiber as reinforcing filler in cornstarch-based biocomposites. *Int J Biol Macromol*. 2019;139:596-604. doi:10.1016/j.ijbiomac.2019.08.015
18. Bertini F, Canetti M, Cacciamani A, Elegir G, Orlandi M, Zoia L. Effect of ligno-derivatives on thermal properties and degradation behavior of poly(3-hydroxybutyrate)-based biocomposites. *Polym Degrad Stab*. 2012;97:1979-1987. doi:10.1016/j.polymdegradstab.2012.03.009
19. Ramos M, Dominici F, Luzi F, et al. Effect of almond shell waste on physicochemical properties of polyester-based biocomposites. *Polymers*. 2020;12(4):835. doi:10.3390/polym12040835
20. Kalitaa NK, Damare NA, Hazarikaa D, Bhagabati P, Kalamdhadc A, Katiya V. Biodegradation and characterization study of compostable PLA bioplastic containing algae biomass as potential degradation accelerator. *Environ Chall*. 2021;3:100067. doi:10.1016/j.envc.2021.100067
21. Campos A, Marconcini JM, Martins-Franchetti SM, Mattoso LHC. The influence of UV-C irradiation on the properties of thermoplastic starch and polycaprolactone biocomposite with sisal bleached fibers. *Polym Deg Stab*. 2012;97:1948-1955. doi:10.1016/j.polymdegradstab.2011.11.010
22. Batista KC, Silva DAK, Coelho LAF, Pezzin SH, Pezzin APT. Soil biodegradation of PHBV/peach palm particles biocomposites. *J Polym Environ*. 2010;18:346-354. doi:10.1007/s10924-010-0238.-4
23. Vasile C, Pamfil D, Râpă M, et al. Study of the soil burial degradation of some PLA/CS biocomposites. *Compos B Eng*. 2018;142:251-262. doi:10.1016/j.compositesb.2018.01.026
24. Wan Ishak WH, Rosli NA, Ahmad I. Infuence of amorphous cellulose on mechanical, thermal, and hydrolytic degradation of poly(lactic acid) biocomposites. *Sci Rep*. 2020;10:11342. doi:10.1038/s41598-020-68274-x
25. Ohkita T, Lee S-H. Thermal degradation and biodegradability of poly(lactic acid)/corn starch biocomposites. *J Appl Polym Sci*. 2006;100:3009-3017. doi:10.1002/app.23425
26. Mittal V, Chaudhry AU, Matsko NB. "True" biocomposites with biopolyesters and date seed powder: mechanical, thermal, and degradation properties. *J Appl Polym Sci*. 2014;131:40816. doi:10.1002/APP.40816
27. Righetti MC, Cinelli P, Mallegni N, et al. Thermal, mechanical, and rheological properties of biocomposites made of poly(lactic acid) and potato pulp powder. *Int J Mol Sci*. 2019;20:675. doi:10.3390/ijms20030675
28. Kalitaa NK, Sarmahb A, Bhasneya SM, Kalamdhadc A, Katiyar V. Demonstrating an ideal compostable plastic using biodegradability kinetics of poly(lactic acid) (PLA) based green biocomposite films under aerobic composting conditions. *Environ Chall*. 2021;3:100030. doi:10.1016/j.envc.2021.100030
29. Alvarez VA, Ruseckaite RA, Vázquez A. Degradation of sisal fibre/mater biocomposites buried in soil. *Polym Deg Stab*. 2006;91(12):3156-3162. doi:10.1016/j.polymdegradstab.2006.07.011
30. Siakeng R, Jawaid M, Asim M, Siengchin S. Accelerated weathering and soil burial effect on biodegradability, colour and texture of coir/pineapple leaf Fibres/PLA biocomposites. *Polymers*. 2020;12:458. doi:10.3390/polym12020458
31. Jia Y, Asoh T-A, Hsu Y-I, Uyama H. Wet strength improvement of starch-based blend films by formation of acetal/hemiacetal bonding. *Polym Deg Stab*. 2020;177:109197. doi:10.1016/j.polymdegradstab.2020.109197
32. Botta L, Titone V, Mistretta MC, et al. PBAT based composites reinforced with microcrystalline cellulose obtained from softwood almond shells. *Polymers*. 2021;13:2643. doi:10.3390/polym13162643
33. Ceraulo M, La Mantia FP, Mistretta MC, Titone V. The use of waste hazelnut shells as a reinforcement in the development of green biocomposites. *Polymers*. 2022;14:2151. doi:10.3390/polym14112151
34. Aliotta L, Vannozzi A, Bonacchi D, Coltelli MB, Lazzeri A. Analysis, development, and sca ling-up of poly(lactic)acid (PLA) biocomposites with hazelnuts shell powder (HSP). *Polymers*. 2021;13:4080. doi:10.3390/polym13234080
35. Botta L, Teresi R, Titone V, Salvaggio G, La Mantia FP, Lopresti F. Use of biochar as filler for biocomposite blown films: structure-processing-properties relationships. *Polymers*. 2021;13:3953. doi:10.3390/polym13223953
36. Averous L, Le Digabel F. Properties of biocomposites based on lignocellulosic fillers. *Carbohydr Polym*. 2006;66:480-493. doi:10.1016/j.carbpol.2006.04.004
37. Scaffaro R, Citarrella MC, Gulino EF. Opuntia Ficus Indica based green composites for NPK fertilizer controlled release produced by compression molding and fused deposition modeling. *Compos – A: Appl*. 2022;159:107030. doi:10.1016/j.compositesa.2022.107030
38. Scaffaro R, Maio A, Gulino EF, Alaimo G, Morreale M. Green composites based on PLA and agricultural or marine waste prepared by FDM. *Polymers*. 2021;13:1361. doi:10.3390/polym13091361
39. Botta L, Titone V, Teresi R, et al. Biocomposite PBAT/lignin blown films with enhanced photo-stability. *Int J Biol Macromol*. 2022;217:161-170. doi:10.1016/j.ijbiomac.2022.07.048
40. Gardette M, Therias S, Gardette JL, Murariu M, Dubois F. Photooxidation of polylactide/calcium sulphate composites. *Polym Deg Stab*. 2011;96:616-623. doi:10.1016/j.polymdegradstab.2010.12.023
41. Rizzarelli P, Puglisi C, Montaudo G. Soil burial and enzymatic degradation in solution of aliphatic co-polyesters. *Polym Degrad Stab*. 2004;85:855-863. doi:10.1016/j.polymdegradstab.2004.03.022
42. Rapisarda M, Mistretta MC, Scopelliti M, Leanza M, La Mantia FP, Rizzarelli P. Influence of calcium carbonate nanoparticles on the soil burial degradation of polybutyleneadipate-

co-cutylenetherephthalate films. *Nanomaterials*. 2022;12:2275. doi:10.3390/nano12132275

43. Zuliani A, Rapisarda M, Chelazzi D, Baglioni P, Rizzarelli P. Synthesis, characterization, and soil burial degradation of bio-based polyurethanes. *Polymers*. 2022;14:4948. doi:10.3390/polym14224948
44. Rizzarelli P, Piredda G, La Carta S, et al. Characterization and laser-induced degradation of a medical grade polylactide. *Polym Degrad Stab*. 2019;169:108991. doi:10.1016/j.polymdegradstab.2019.108991
45. Partini M, Pantani R. FTIR analysis of hydrolysis in aliphatic polyesters. *Polym Degrad Stab*. 2007;92:1491-1497. doi:10.1016/j.polymdegradstab.2007.05.009
46. Emadian SM, Onay TT, Demirel B. Biodegradation of bioplastics in natural environments. *Waste Manag*. 2017;59:526-536. doi:10.1016/j.wasman.2016.10.006
47. Eubeler JP, Zok S, Bernhard M, Knepper TP. Environmental biodegradation of synthetic polymers I. Test methodologies and procedures. *TrAc Trends Anal Chem*. 2009;28:1057-1072. doi:10.1016/j.trac.2009.06.007
48. Rizzarelli P, Rapisarda M, Ascione L, Degli Innocenti F, La Mantia FP. Influence of photo-oxidation on the performance and soil degradation of oxo- and biodegradable polymer-based items for agricultural applications. *Polym Degrad Stab*. 2021;188:109578. doi:10.1016/j.polymdegradstab.2021.109578
49. Rapisarda M, La Mantia FP, Ceraulo M, et al. Photo-oxidative and soil burial degradation of irrigation tubes based on biodegradable polymer blends. *Polymers*. 2019;11:1489. doi:10.3390/polym11091489
50. La Mantia F, Ascione L, Mistretta MC, Rapisarda M, Rizzarelli P. Comparative investigation on the soil burial degradation behaviour of polymer films for agriculture before and after photo-oxidation. *Polymers*. 2020;12:753. doi:10.3390/polym12040753

SUPPORTING INFORMATION

Additional supporting information can be found online in the Supporting Information section at the end of this article.

How to cite this article: Baiamonte M, Rapisarda M, Mistretta MC, Impallomeni G, La Mantia FP, Rizzarelli P. Wood flour and hazelnut shells polylactide-based biocomposites for packaging applications: Characterization, photo-oxidation, and compost burial degradation. *Polym Compos*. 2024;45(11):9802-9818. doi:10.1002/pc.28439